Geometrical optimization of an ultrasonic tactile plate for surface texture rendering

Peter Sergeant, Frédéric Giraud, Betty Lemaire-Semail

Geometrical optimization of an ultrasonic tactile plate for surface texture rendering

Peter Sergeant[a,b], Frédéric Giraud[c], Betty Lemaire-Semail[c]

[a] *Dept. of Electrical Energy, Systems and Automation, Ghent University, Sint-Pietersnieuwstraat 41, B-9000 Ghent, Belgium*
[b] *Dept. of Electrotechnology, Faculty of Applied Engineering Sciences, University College Ghent, Schoonmeersstraat 52, B-9000 Ghent, Belgium*
[c] *Univ Lille Nord de France, F-59000 Lille, France; L2EP F-59000 Villeneuve d'Ascq, France*

Abstract

The Tactile plate consists of piezo-ceramics glued on a copper-beryllium resonator. Its purpose is to create programmable tactile sensations, which give the illusion of finely textured surfaces. The illusion originates from the variable friction between a finger and the vibrating resonator, caused by the squeeze film effect. In order to obtain a maximal deflection of the plate for a minimal supply voltage, an optimization is carried out of the length, thickness, and width of both the resonator and the ceramics. Constraints are realistic geometrical dimensions, a resonance frequency of at least 25 kHz, and a low supply voltage. The plate is modelled by both an analytical and a numerical model. The maximal dynamical deflection per volt was achieved with thin piezo ceramics (0.5 mm) at the minimal frequency of 25 kHz. A high deflection can be obtained in a wide range of the resonator length. With increasing length, the optimal resonator thickness increases too. The plate width seems to have little influence. Experiments are carried out on two plates with different geometry.

Key words: Piezo-electricity, Optimization, Tactile Plate
PACS: 77.65.Fs, 02.60.Pn, 02.70.Dh

1. Introduction

A tactile stimulator provides information to a user through the sense of touch. It can be used as a texture or shape simulator into an immersive virtual environment, or as an input–output tactile pad as those found on any new electronic hand-held device. To achieve that, some stimulators try to create the illusion of touching a virtual shape by using pins array. These devices suffer from their large bulk size which increases with the resolution with which the virtual shape is simulated[1]: the touching area is thus limited, and the user's fingertip can't move with a free motion. To tackle this problem, an other proposal is deluding a user by simulating the *effect* of the shape on the fingertip. Pin array is then used to recreate lateral stretches of the skin appearing when a user is touching a bump or a hole[2].

The tactile stimulator studied in this paper belongs to another family of tactile devices. It is named "the tactile plate" as it uses a vibrating plate to produce tactile stimuli. However, the vibration is not used to directly create stimuli, but to modify the friction between fingertip and the plate. The working principle of the tactile plate is based on the squeeze film effect: if the thin layer of air between the plate and the finger is compressed and expanded very rapidly by the vibration, then an overpressure is generated that tries to lift the finger. The squeeze film effect reduces the friction between the plate and the finger during the vibration of the plate. Several experimental studies have shown that it is possible to create tactile feedback with this operating principle. For example [3] modifies roughness perception of samples of sand papers, while [4] has shown that it is possible to give the illusion of touching finely textured surfaces with a programmable spatial period. The main advantage of such devices is that they allow a free motion of the fingertip on the virtual surface. By this way, user's movement is not constrained: interaction between the user and the device is thus natural.

There exist several designs which produce tactile feedback based on friction reduction: [3] uses two langevin transducers to make a thin iron plate vibrate; [5] uses a disc shape ring resonator to reduce the size of the device. In [4], a rectangular copper plate with thin piezo-electric elements bonded on it was designed. This solution uses a standing wave with multiple wavelength propagating on top of the device. This design allows a large exploration area, with a small thickness and thus results in size reduction. However, in each case, squeeze film effect is effectual if the vibration amplitude is in the order of several micrometers at 25kHz or above [6].

To complete surface texture rendering, the friction coefficient has to be a function of fingertip's position, and

Email addresses: Peter.Sergeant@ugent.be (Peter Sergeant), Frederic.Giraud@polytech-lille.fr (Frédéric Giraud), Betty.Semail@polytech-lille.fr (Betty Lemaire-Semail)

then we need its precise and accurate control. For example, gratings can be simulated by switching between a high friction level, to a smaller one. Thus, the plate's capability to produce high vibration amplitude is a key feature for tactile simulation since smaller friction level is achieved with larger vibration amplitude. Previous work in [6] has shown that friction reduction depends on plate's original roughness, but it's also found that a value af $300nm$ can be considered as a minimum deflection below which friction reduction is too small.

Optimization of the tactile plate is required in order to obtain a large vibration amplitude for a low supply voltage, without violating the several constraints. These constraints are 1) realistic dimensions of the plate 2) resonance frequency above 25 kHz to have the squeeze film effect 3) low supply voltage for safety reasons and for low power consumption to avoid heating of the plate. The optimization uses a 3D numerical model in combination with an analytical model to accelerate the computation.

After explaining these models in section 2, we analyze the influence of several geometrical parameters in section 3 in order to find some general design rules, similar to [7, 8, 9]. Next to geometrical parameters, also the issue of damping is discussed. Experiments are carried out for two geometries (section 4). Finally, the conclusion summarizes which parameters are important to develop an efficient tactile plate.

2. Efficient optimization requires two models of the tactile plate

2.1. Analytical model

The first model is an analytical model based on the one in [6]. It is recalled in the following paragraphs. Firstly, the static deflection is studied on a simply-supported beam (see Fig. 1) whose length is half of the wavelength λ. Secondly, the dynamic deflection is calculated. Thirdly, the resonance frequency is determined, and finally, the cost calculation is explained.

2.1.1. Static deflection

The modelled beam (Fig. 1) consists of a resonator with thickness h_i in copper beryllium – the mechanical resonator – glued to a layer of piezoelectric ceramics with thickness h_p. It is assumed that the thickness of the glue is zero and that the strains are continuous on the resonator-piezoelectric ceramic interface. The beams length is $\lambda/2$ and its width b.
Firstly, the displacement vector in the cartesian frame is described using the Bernoulli-Euler theory [10]

$$U = \begin{pmatrix} u \\ v \\ w \end{pmatrix} = \begin{pmatrix} (z_0 - z)\frac{\delta w}{\delta x} \\ (z_0 - z)\frac{\delta w}{\delta y} \\ w(x,y,t) \end{pmatrix} \tag{1}$$

where $w(x,y,t)$ represents the displacement along the z axis, and z_0 the neutral plan ordinate, which distinguishes the compressed and the stretched zones in the plate.

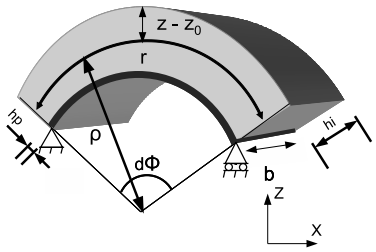

Figure 1: Half-wavelength beam which bends by contracting the piezoceramics.

The radius of curvature, ρ, due to bending moments caused by contraction of the piezoceramic, can be determined from the resulting stresses and strains in the composite beam (Fig. 1). The plate does not vibrate according to a planar movement but bends. In fact, it is easier to realize bending deformation than planar deformation.

The resonator is considered to be isotropic and the stress T_i can be expressed by the reduced form as follows:

$$T_i = E_i S_{xx} \tag{2}$$

where E_i is the Young modulus of the Copper Beryllium and where $S_{xx}(z)$ is the strain component along the x-axis acting on the plane normal to the x-axis. As for the piezoelectric part of the plate, the constitutive relationships between the stress, strain and applied fields can be expressed in terms of the piezoelectric stress relations

$$T_p = c^E S - e^t \mathcal{E} \qquad D = eS + \epsilon^S \mathcal{E} \tag{3}$$

where $\mathcal{E}$ is the electric field intensity vector and D is the electric flux density vector. c^E, e and ϵ^S are respectively the elastic constants short circuit matrix, the voltage coefficients and the dielectric constants matrixes.

Finally, the stress distributions on the x-faces due to an applied electric field in the z-direction can be written as follows:

$$T_{xx}(z) = \begin{cases} E_i S_{xx}(z) & h_\mathrm{p} < z < h_\mathrm{p} + h_\mathrm{i} \\ c^E_{11_p} S_{xx} - d_{31} c^E_{11_p} \mathcal{E}_z & 0 < z < h_\mathrm{p} \end{cases} \tag{4}$$

where $e^t = d_{31} c^E_{11_p}$

Considering that no external force acts on this structure, we can deduce that curve c can be expressed as follows [6]:

$$c = \frac{1}{\rho} = \frac{\mathrm{d}^2 w}{\mathrm{d}x^2} = \frac{3}{2}\frac{d_{31}\mathcal{E}_z}{h_\mathrm{p} a} \tag{5}$$

where

$$\frac{1}{a} = \frac{1 - 2f_0}{1 - 3f_0 + 3f_0^2 + \alpha(3\beta + 3\beta^2 + \beta^3 - 6\beta f_0 - 3\beta^2 f_0 + 3\beta f_0^2)}$$

and

$$\alpha = \frac{E_i}{c^E_{11_p}} \quad , \beta = \frac{h_\mathrm{i}}{h_\mathrm{p}}, \quad f_0 = \frac{zo}{h_\mathrm{p}} \tag{6}$$

By taking into account the boundary conditions of a simply-supported beam and by integrating equation (5) twice, we obtain the displacement profile:

$$w(x) = \frac{3}{4}\frac{d_{31}\mathcal{E}_z}{h_\mathrm{p} a}\left(x^2 - \frac{\lambda}{2}x\right) \tag{7}$$

and the static deflection $w_\mathrm{max} = w(\lambda/4)$ at $\frac{\lambda}{4}$ is given by:

$$w_\mathrm{max} = \frac{-3}{16}\frac{d_{31}\mathcal{E}_z}{h_\mathrm{p}}\frac{(\lambda/2)^2}{a} = -\frac{3}{16}\frac{d_{31}V_\mathrm{z}}{h_\mathrm{p}^2}\frac{(\lambda/2)^2}{a} \tag{8}$$

where V_z is the voltage applied between the piezo-ceramic electrodes.

2.1.2. Determination of the dynamic deflection

In order to increase the deflection, we work at resonance frequency. This explains why, in this subsection, we must determine the dynamic deflection, which is the static deflection times the dynamic amplification factor.

The dynamic amplification factor $Q = Q_m U_\mathrm{mono}/U_\mathrm{piezo}$ is the mechanical quality factor Q_m of the piezoceramics balanced by the ratio of the strain energy of the entire monomorph U_mono to the strain energy of the piezoelectric layer U_piezo [11].

The stored elastic energy in the piezoelectric layer is

$$U_\mathrm{piezo} = \frac{\lambda b}{2}\frac{1}{2}\int_z S_{xx}T_{s_\mathrm{piezo}}\,\mathrm{d}z \tag{9}$$

and the stored elastic energy in the entire monomorph is given by

$$U_\mathrm{mono} = \frac{\lambda b}{2}\frac{1}{2}\int_z S_{xx}(T_{s_\mathrm{piezo}} + T_{s_\mathrm{reson}})\,dz \tag{10}$$

From [6], we can deduce the stored energy as a function of the material properties and the geometrical dimension of the structure:

$$U_\mathrm{piezo} = \frac{\lambda b}{4}\int_0^{h_\mathrm{p}} c_{11_p}^E S_{xx}^2\,\mathrm{d}z \tag{11}$$

$$= \frac{3}{16}\lambda b h_\mathrm{p} d_{31}^2 \mathcal{E}_z^2 c_{11_p}^E \frac{1 - 3f_0 + 3f_0^2}{a^2} \tag{12}$$

and

$$U_\mathrm{mono} = \frac{\lambda b}{4}\int_0^{h_\mathrm{p}} d_{31} c_{11_p}^E \mathcal{E}_z\left(\frac{z - z_0}{\rho}\right)\mathrm{d}z \tag{13}$$

The neutral line ordinate z_0 is found by expressing that the sum of the stresses at both sides of the line equals zero: $0 = \int_z S_{xx}(T_{s_\mathrm{piezo}} + T_{s_\mathrm{reson}})\,\mathrm{d}z$, resulting in

$$z_0 = \frac{h_\mathrm{p}(1 + \alpha\beta^2 + 2\alpha\beta)}{2(1 + \alpha\beta)} \tag{14}$$

Here, we assumed that the materials are purely elastic, i.e. with a null electric field. Then, by inserting (14) into (13), we obtain

$$U_\mathrm{mono} = \frac{3}{16}\lambda b h_\mathrm{p} d_{31}^2 \mathcal{E}_z^2 c_{11_p}^E \frac{1 - 2f_0}{a}$$

Finally, $Q = Q_m \frac{a(1-2f_0)}{1-3f_0+3f_0^2}$ and $w_\mathrm{dyn} = w\left(\frac{\lambda}{4}\right)Q$:

$$w_\mathrm{dyn} = Q_m \frac{-3}{16}\frac{d_{31}V_\mathrm{z}}{h_\mathrm{p}^2}\frac{\lambda^2}{4}\frac{1 - 2f_0}{1 - 3f_0 + 3f_0^2} \tag{15}$$

Notice that the deflection in the analytical model is independent of the beam width b.

2.1.3. Determination of the resonance frequency

The resonance frequency f_r is [12, 13]:

$$f_\mathrm{r} = \frac{2\pi}{\lambda^2}\sqrt{\frac{G_\mathrm{b}}{M_\mathrm{b}}} \tag{16}$$

with $G_\mathrm{b} = c_{11_p}^E \int_0^{h_\mathrm{p}} (z - z_0)^2\,\mathrm{d}z + E_\mathrm{i}\int_{h_\mathrm{p}}^{h_\mathrm{p}+h_\mathrm{i}} (z - z_0)^2\,\mathrm{d}z$ the flexional rigidity of the beam in [N.m] and $M_\mathrm{b} = \rho_\mathrm{b} h_\mathrm{b} + \rho_\mathrm{i} h_\mathrm{i}$ the total mass per length in [kg/m^2].

2.1.4. Analytical cost function

For use in optimization routines, a cost function is created that contains the analytical model.

The objective is to have a maximal deflection per volt supply voltage. This means that the cost is given by (15) with V_z equal to a constant voltage. Since users directly touch the tactile plate. We chose $V_\mathrm{z} = 15V$ because it is a safe voltage level.

The six parameters to optimize are the length, thickness and width of the resonator and the ceramics. Nevertheless, the cost function has only three inputs: the wavelength λ, the resonator thickness h_i, and the piezo-ceramics thickness h_p. As the number of piezo-ceramics $n = 7$ and the space between adjacent ceramics δ are constant, the wavelength also determines two additional parameters: the length l_p of the ceramics and the length L of the resonator as shown in Table 1. The two remaining parameters – the width of the ceramics and the resonator – are equal and denoted by b. However, the width b cannot be optimized in the analytical model, because the cost (15) does not depend on b.

2.2. Numerical model

2.2.1. Finite element model

The second model is a 3D linear finite element model (FEM) in the software package Comsol. The number of degrees of freedom varies between 10^4 and 10^5, depending on the geometry. The modelled geometry and boundary conditions are shown in Fig. 2: the FEM geometry is only a quarter of the tactile plate because symmetry is exploited both along the x- and the y-direction.

The model in Comsol was validated by comparing it with the Ansys model in [6] for the same plate geometry. The geometry studied in the following sections is however slightly different from the one in the cited paper: the length of the resonator is increased by $\lambda/8$ at both ends in comparison with the plate in [6]. The aim of the modification is to slightly modify the wavelength at resonance so that $\lambda = 2(l_\mathrm{p} + \delta)$. This means that the nodes of the

Table 1: Geometric and material properties of the tactile plate

Resonator		
Wavelength	λ	$15 < \lambda < 40$ mm
Number ceramics along x	n	7
Gap between ceramics	δ	1.0 mm
Length	L	$\frac{2n+1}{4}\lambda \rightarrow 56 < L < 150$ mm
Thickness	h_i	$0.2 < h_\mathrm{i} < 3$ mm
Width	b	$0.03 < b < 0.10$ m
Young modulus	E_i	123×10^9 N.m^{-2}
Mass density	ρ_i	8250 kg/m^3
Poisson coefficient	ν_i	0.31
Ceramic		
Length	l_p	$\frac{\lambda}{2} - \delta \rightarrow 6.5 < l_\mathrm{p} < 19$ mm
Thickness	h_p	0.5 mm, 1.0 mm or 2.0 mm
Piezoelectric constant	e_{31_p}	-4.9 C.m^{-2}
Elastic constant	$c^E_{11_p}$	6.79×10^{10} N.m^{-2}
Charge coefficient	d_{31}	-247×10^{-12} m.V^{-1}
Mechanical quality factor	Q_m	60
Mass density	ρ_p	7410 kg/m^3
Poisson coefficient	ν_p	0.33

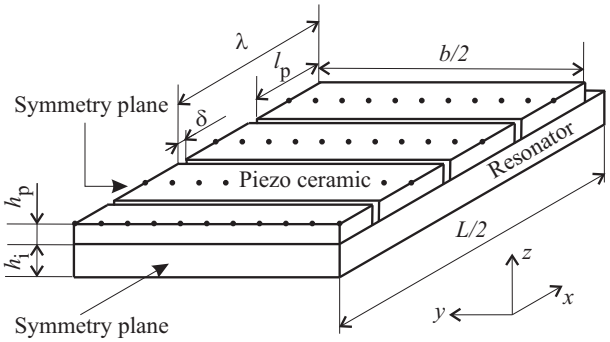

Figure 2: Geometry of the tactile plate in the 3D FEM, which is only one quarter of the entire plate. The dots represent the points used to determine the average deflection (antinodes). Dimensions and material properties can be found in Table 1.

standing wave are exactly between adjacent ceramics (at $x = k(l_\mathrm{p} + \delta)/2, k = -7, -5, ..., 7$) and the anti-nodes are exactly in the middle of the ceramics ($k = -6, -4, ..., 6$). This increases the efficiency of the piezo-ceramics to generate a strong vibration.

In contrast with the analytical model, the numerical model has also transverse resonance modes for some geometries. Fig. 3 shows that a small modification of the plate width b can make the difference between a pure longitudinal resonance mode, and a mixed longitudinal/transverse resonance mode.

2.2.2. Numerical cost function

The cost function containing the parametrized numerical model should be able to determine w_dyn for each possible geometry of the tactile plate. The resonance frequencies and the corresponding resonance modes (along the x-direction and/or along the transverse y-direction) are not known a priori. To tackle this problem, the cost function is organized as follows. After creating the geometry and the mesh, the cost function searches for eigenfrequencies.

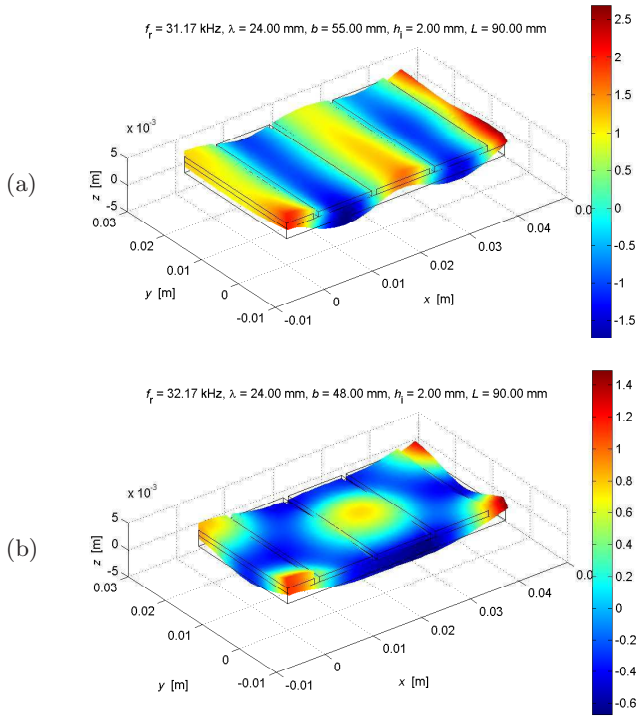

Figure 3: Deformation in μm of (one quarter of) the tactile plate with $\lambda = 24$ mm, $h_\mathrm{i} = 2.0$ mm, $h_\mathrm{p} = 1.0$ mm. In (a), the width b is 55 mm giving rise to a pure resonance mode in x-direction. In (b), the width b is 48 mm, resulting in an additional transverse resonance mode

Then, it performs a time-harmonic FEM analysis for each considered eigenfrequency. The damping is set by a quality factor Q. Next, for each time-harmonic model, the deflection is calculated as an average of the deflection $|w_\mathrm{dyn}|$ in the 44 relevant points shown in Fig. 2. The points are at the positions where in theory the maximal deflection of the standing wave occurs. Finally, among all considered resonance modes, the cost function selects the resonance mode that has the highest deflection.

The analytical model is very useful to limit the calculation time of the FEM model, because it estimates the resonance frequency f_r. Without a priori information about f_r, all resonance modes in the considered frequency range should be evaluated in a time-harmonic FEM evaluation. By using the predicted f_r from the analytical model for the same inputs, the numerical cost function has to evaluate the 3D FEM only for a few resonance frequencies close to the predicted f_r. In practice, evaluating the six "nearest" eigenfrequencies seemed to be sufficient for the whole range of h_i and λ in Table 1. On a 2.4 GHz CPU, the evaluation time of the numerical cost function considering six eigenfrequencies is between 50 s and 650 s, depending on the number of degrees of freedom.

The cost of the numerical cost function is the same as for the analytical model: the dynamical deflection for $V_\mathrm{z} = 15$ V. The function has four inputs: the same three inputs λ, h_i, and h_p as the analytical model, and the plate

width b as an additional input.

2.3. Optimization

Both the analytical and the numerical cost functions are optimized, in order to see the difference between both functions. The optimization routines try to maximize the deflection for a given voltage by iteratively evaluating the analytical or the numerical cost function. The optimization routines consider two real input parameters λ and h_i, and one discrete parameter h_p: not all thicknesses are commercially available. In order to cope with the mixed discrete/real optimization problem, the optimization for the two real parameters only is repeated for several values of h_p. The parameter b is not included because it has no or few influence on the cost. The influence of b in the numerical model is shown in section 3.3.

From the three constraints mentioned in the introduction, the first one – realistic dimensions – is achieved by setting the lower and upper boundaries of the parameters as given in Table 1; the second one – $f_\mathrm{r} > 25$ kHz – is programmed as a constraint in the optimization routine; the third one is taken into account by choosing a constant, safe V_z of 15 V.

The analytical cost function is optimized by the Matlab function *fmincon*, which is a gradient based technique.

For the numerical cost function, two optimization routines are compared. The first one is also *fmincon*, wherefor the starting value is the optimum of the analytical cost function. The second routine is the Space Mapping technique [14, 15, 16] which is an efficient optimization technique if a fast but inaccurate model and a slow but accurate model are available. This technique combines both models to take advantage of the speed of the fast model without loosing the accuracy of the slow model. The analytical model is useful as fast inaccurate model and the numerical model as slow accurate model. The analytical model speeds up the optimization in two ways: on the one hand, by reducing the number of numerical cost function evaluations in the space mapping algorithm, and on the other hand by limiting the number of resonance frequencies to investigate in the numerical cost function.

3. Effects of geometrical parameters and damping, simulated by both models

3.1. Resonator thickness and length of the piezo ceramics

For all simulations and experiments, the resonator is made from a copper-beryllium alloy, and the ceramics are lead titanate zirconate ceramics type PI-91, manufactured by Saint-Gobain Quartz. The characteristics of the materials are given in Table 1. Additional properties of the ceramics can be found in [6]. As already mentioned, the voltage supply of the piezo-ceramics is set to 15 V in order to avoid dangerous voltages. For this section, the quality factor Q is chosen constant and equal to 54. This value is obtained from experiments on the plate from [6] with $\lambda = 24$ mm, $h_\mathrm{i} = 2.0$ mm, $h_\mathrm{p} = 1.0$ mm and $b = 49$ mm. In the following sections, this plate is called the "original tactile plate". For the chosen Q-value, the simulated dynamical deflection of the original plate equals the experimentally observed one.

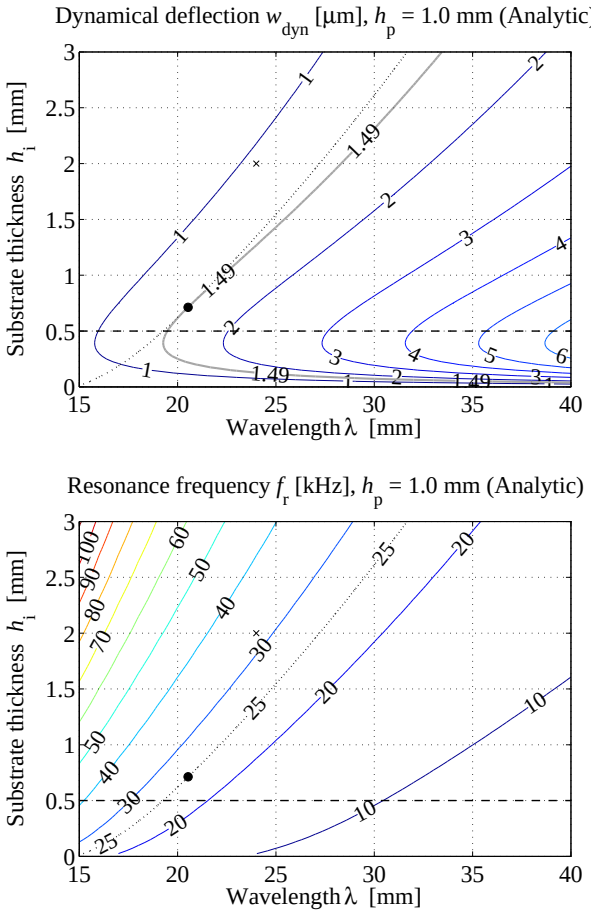

Figure 4: Contour lines of equal dynamical deflection in (a) and equal resonance frequency in (b) found by the analytical model for $h_\mathrm{p} = 1.0$ mm and $Q = 54$. The black circle shows the optimum ($\lambda^* = 20.54$ mm, $h_\mathrm{i}^* = 0.712$ mm, $w_\mathrm{dyn} = 1.4908$ μm, $f_\mathrm{r} = 25.00$ kHz), and the cross shows the original plate ($\lambda = 24.00$ mm, $h_\mathrm{i} = 2.00$ mm, $w_\mathrm{dyn} = 1.070$ μm, $f_\mathrm{r} = 32.13$ kHz). The dotted line indicates the minimal frequency of 25 kHz and the dashed line indicates the minimal resonator thickness of 0.5 mm. An additional contour line is added at $w_\mathrm{dyn} = 1.4908$ μm to indicate the points with equal deflection as the optimum.

For a piezo-ceramics thickness of 1.0 mm, the deflection of the beam and its resonance frequency calculated by the analytical cost function are shown as a function of the wavelength λ and the resonator thickness h_i in Fig. 4. It is recalled that the results of the analytical model are independent of the plate width b, and that the wavelength is related to the length $L = (2n+1)\lambda/4$ of the plate, and to the length of the piezo-ceramics: $l_\mathrm{p} = \lambda/2 - \delta$ with δ the separation between adjacent ceramics. When moving to the right in the figure, the total plate length L increases; when moving upward, the total thickness increases. High deflections can be found in the lower right corner, but here

the resonance frequency is below 25 kHz. Because of the constraint that the frequency should be above 25 kHz to produce squeeze film effect, the plate dimensions should be chosen in the region left of the dotted line. Furthermore, the minimal resonator thickness should be 0.5 mm for practical reasons, so that the optimum is not allowed to be below the dashed line. The minimization results in the point indicated by a circle in Fig. 4. This is the point where the curve with frequency equal to 25 kHz (dotted line) is tangential to the curve with deflection equal to 1.49 μm (thick gray line).

The results of the numerical model are shown in Fig. 5 for $b = 49$ mm. The contour lines of equal resonance frequencies correspond well with the ones of the analytical model; the contour lines of equal deflections are less smooth. This is caused by transverse modes that influence the determination of the average deflection. These modes are not taken into account by the analytical model.

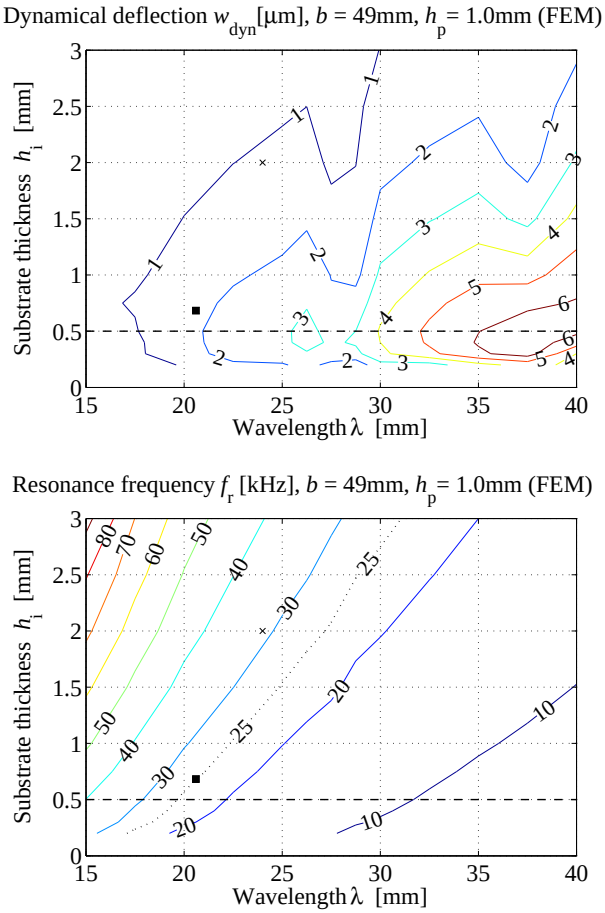

Figure 5: Contour lines of equal dynamical deflection in (a) and equal resonance frequency in (b) found by the numerical model for $h_p = 1.0$ mm and $Q = 54$. The square shows the optimum ($\lambda^* = 20.60$ mm, $h_i^* = 0.683$ mm, $w_{dyn} = 1.8417$ μm, $f_r = 25.04$ kHz). The original plate indicated by the cross has $\lambda = 24.00$ mm, $h_i = 2.00$ mm, $w_{dyn} = 1.151$ μm, $f_r = 31.17$ kHz

The optima of the analytical cost function (circle in Fig. 4) and of the numerical cost function (square in Fig. 5) are very close to each other. In spite of the good correspondence, it is not a good idea to design a tactile plate using the analytical cost function only. The numerical model is useful in order to avoid possible undesired transverse modes that are not predicted by the analytical model. For the analytical cost function, the optimum was found quickly by the Matlab routine *fmincon*. The numerical cost function was also optimized by *fmincon*, using the optimal solution of the analytical model as a starting value. Although the "landscape" of the numerical cost function is not very smooth, the gradient based algorithm was able to find the optimum in 48 evaluations. When using space mapping, the optimization required only four evaluations of the numerical cost function. In addition, four optimizations were needed of the analytical cost function, but the time to *optimize* the analytical cost function is negligible compared to the time to *evaluate* the numerical model. Although the total CPU time is ten times less than for the conventional gradient approach, the optimum found was almost the same (difference less than 0.1 mm).

3.2. Thickness of the piezo-ceramics

The influence of the thickness can be seen by comparing the deflection for $h_p = 1.0$ mm in Fig. 4 and Fig. 5, with the deflection for $h_p = 2.0$ mm in Fig. 6 and for $h_p = 0.5$ mm in Fig. 7 and Fig. 8. The supplied voltage and the Q-factor are unchanged.

The deflection decreases for thicker piezo-ceramics. The contour lines of equal deflection have a bend that occurs at a thickness that is roughly half of the ceramics thickness. If the wavelength increases, the corresponding h_i that generates the highest deflection increases too. The optimum h_i increases if h_p increases: for $h_p = 0.5$ mm it is on the minimal allowed thickness. For $h_p = 1$ mm, it is at 0.7 mm, and for $h_p = 2$ mm, it is on 1.5 mm. Also the optimal wavelength increases for increasing h_p. To summarize: if the piezo thickness increases, then all other dimensions of the plate should increase also. Nevertheless, the amplitude of deflection reduces with increasing h_p.

The frequency decreases only a bit with increasing h_p. For all three considered thicknesses, the optimum has a resonance frequency of 25 kHz. Higher frequencies always have lower deflections.

3.3. Plate width

In Fig. 9, the dashed line shows that in the analytical model, the plate width b has no influence on the deflection, neither on the frequency. The numerical model shows that the deflection and the resonance frequency slightly decrease for low $b < 40$ mm. The analytical model does not predict this decrease. Indeed, for small plate widths, the analytical model is not valid as it assumes that the plate thickness $h_i + h_p$ is much smaller than its length and width. The deflection should in theory be constant for $b > 40$ mm. The deflection obtained by the numerical model as a function of b is not smooth at all. This is caused by transverse

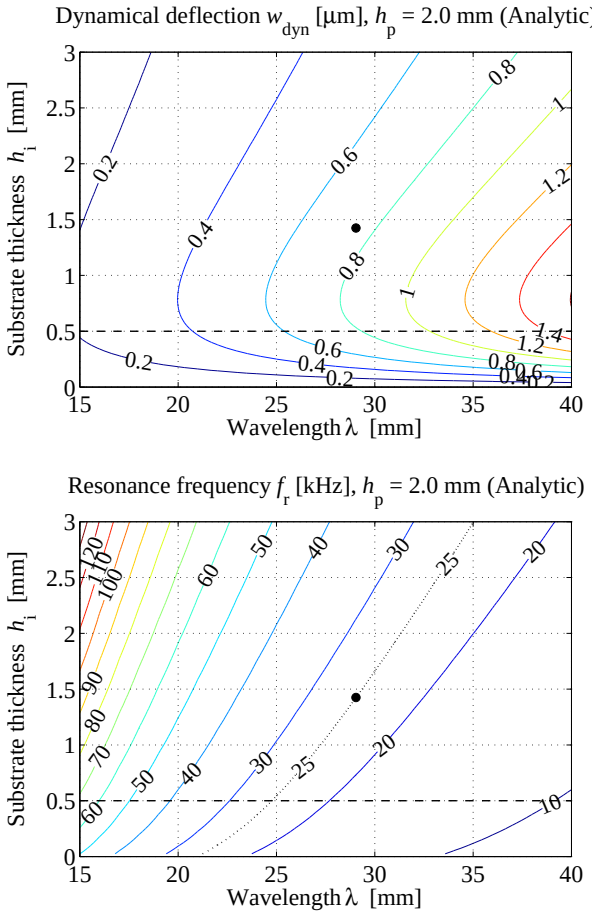

Figure 6: Contour lines of equal dynamical deflection in (a) and equal resonance frequency in (b) found by the analytical model for $h_p = 2.0$ mm. The circle shows the position of the optimum ($\lambda^* = 29.04$ mm, $h_i^* = 1.425$ mm, $w_{dyn} = 0.7454$ μm, $f_r = 25.00$ kHz)

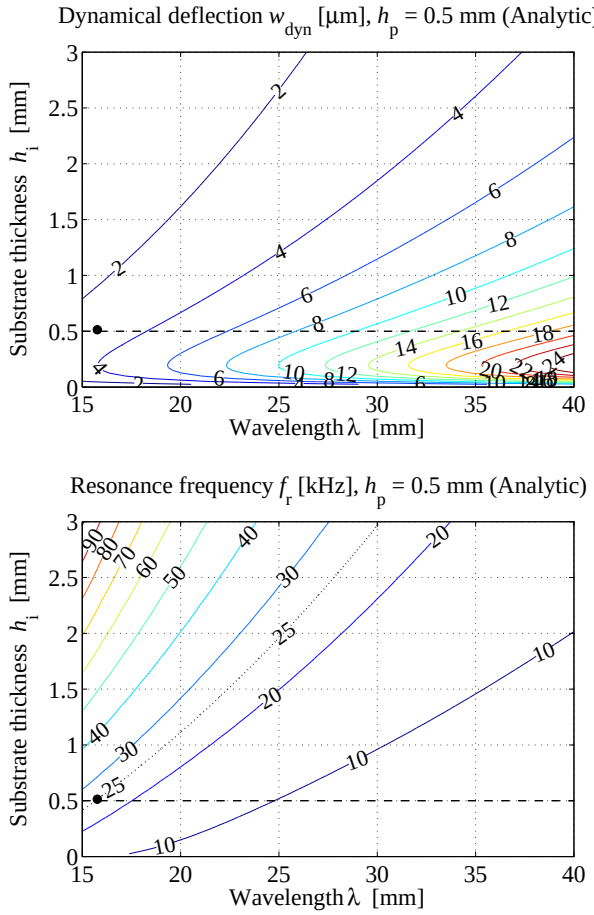

Figure 7: Contour lines of equal dynamical deflection in (a) and equal resonance frequency in (b) found by the analytical model for $h_p = 1.0$ mm and $Q = 54$. The circle shows the position of the optimum ($\lambda^* = 15.76$ mm, $h_i^* = 0.500$ mm, $w_{dyn} = 2.9308$ mm, $f_r = 25.00$ kHz), which has h_i^* and f_r equal to the constraints of 0.5 mm and 25 kHz resp. (dashed lines). If the constraint on h_i is removed, the optimum is at $\lambda^* = 14.52$ mm, $h_i^* = 0.356$ mm, $w_{dyn} = 2.9814$ μm, $f_r = 25.00$ kHz.

modes that disturb the efficient deformation of the plate – see also Fig. 3. In the hypothetic case without these transverse modes, the deflection would be given by a curve that connects all the tops of the curve. This curve would predict a deflection that corresponds well with the analytical one. The resonance frequency is not much affected by the transverse modes, as can be observed in Fig. 9, taking into account the detailed scale.

3.4. Damping

The Q-factor for the damping was experimentally determined based on the deflection of the original tactile plate. In the previous sections, the same Q-factor of 54 was chosen also for other geometries. For the optimized plate with $h_p = 0.5$ mm (black square in Fig. 8), this results in the deflection w_{dyn} shown in Fig. 10 as a function of time and in Fig. 11 as a function of the frequency. The maximal deflection is about 4 μm and the time constant is approximately 1 ms.

However, according to literature, the Q-factor decreases with the vibration velocity of the piezo-ceramics. The figure 3.8 in [17] shows for a piezo-ceramic without resonator a Q-factor that strongly decreases as a function of the displacement speed v: Q is about 2000 for $v < 0.1$ m/s, and decreases rapidly if v increases: Q is about 200 at $v = 0.25$ m/s. To obtain a more realistic map of the deflection $w_{dyn}(\lambda, h_i)$, the Q-factor was experimentally measured as a function of v for the original setup. The result – displayed in Fig. 12 – is similar to [17] for v >0.2 m/s, and much lower for smaller v. The latter is due to the additional damping by the glue that is not present in the cited figure.

Modifying the map with a variable Q-factor gives rise to Fig. 13. The resonance frequency is not shown because it remains the same as in Fig. 5. The deflection remains the same for the original plate (indicated by a cross). The deflection becomes much lower for most other geometries, but the position of the optimum doesn't change.

In some applications, a prescribed deflection should be obtained with the lowest possible voltage. Fig. 13 shows

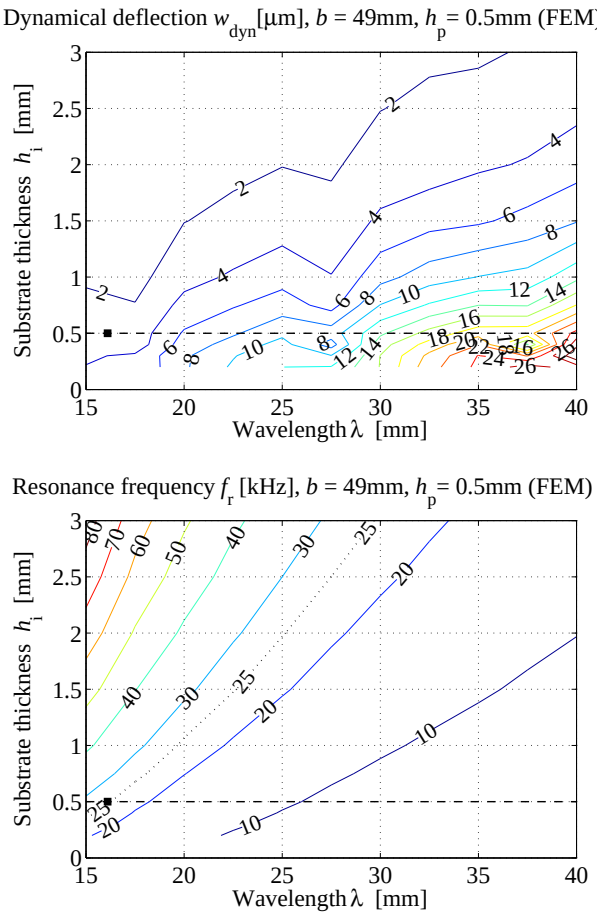

Figure 8: Contour lines of equal dynamical deflection in (a) and equal resonance frequency in (b) found by the numerical model for $h_\mathrm{p} = 0.5$ mm and $Q = 54$. The black square shows the position of the optimum ($\lambda^* = 16.10$ mm, $h_\mathrm{i}^* = 0.500$ mm, $w_\mathrm{dyn} = 3.9743$ μm, $f_\mathrm{r} = 25.07$ kHz).

the voltage needed to obtain a deflection of 1.15 μm. For the original plate, evidently, the required voltage is 15 V.

Changing the thickness of the piezo-ceramics results in Fig. 14. The deflection is still larger than for $h_\mathrm{p} = 1$ mm, but the difference is much smaller than with constant Q.

The optimal wavelength and resonator thickness for $h_\mathrm{p} = 1$ mm and 0.5 mm changes only slightly in comparison with the ones for Q constant, but the deflection at the optimum is strongly reduced. This is an important conclusion, because it means that the changes in the damping type has almost no influence on the optimal dimensions of the plate.

4. Experiments

Tactile plates are built up with piezo cells which are bonded on the copper-beryllium substrate. First, a thin layer of Epoxy is spread onto the substrate. Then the cells are precisely positioned. The assembly is pressed, and put into an oven for polymerization of the glue. Figure 15 presents a tactile plate after the polymerization process.

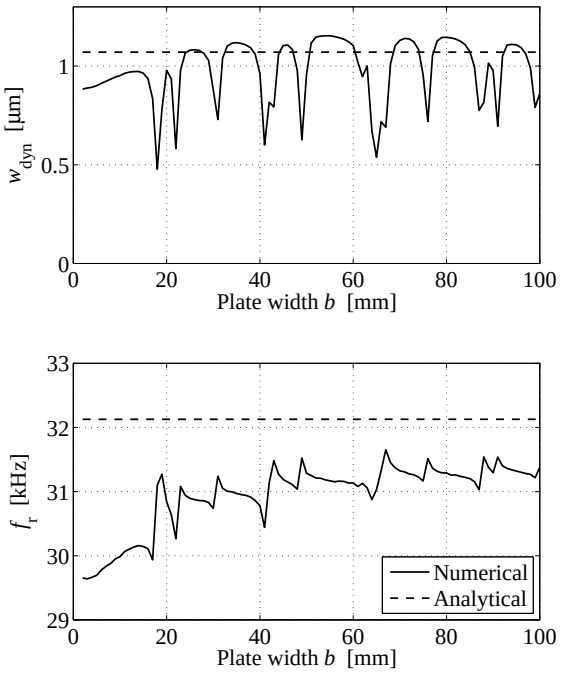

Figure 9: Deflection as a function of the plate width shows the effect of transverse modes for the original configuration. The deformation for $b = 48$ mm and for $b = 55$ mm is shown in Fig. 3.

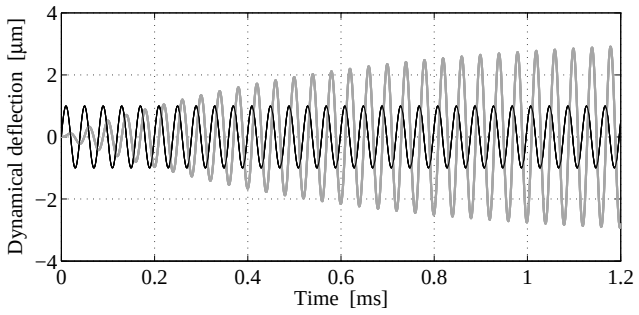

Figure 10: Time simulation at 25070 Hz for the optimized tactile plate with $h_\mathrm{p} = 0.5$ mm, $\lambda^* = 16.10$ mm, $h_\mathrm{i}^* = 0.500$ mm. The gray line shows the average deflection that has at the resonance frequency a phase lag of 90° compared to the applied voltage over the piezo-ceramics (black line). The time constant is approximately 1 ms.

Two tactile plates were manufactured according to optimization's results. However, we could not be supplied with $h_i = 0.673mm$, we have chosen $h_i = 0.75mm$ instead. We name these two plates P1 and P2, and they have the following characteristics respectively:

- P1: $h_p = 1.0mm$, $h_i = 0.75mm$ and $\lambda^* = 20.56mm$,
- P2: $h_p = 0.5mm$, $h_i = 0.5mm$ and $\lambda^* = 15.66mm$.

Dynamical deflection, resonance frequency , and the voltage necessary to reach $1.15\mu m$ were measured. Results are presented in the following paragraphs.

4.1. Experimental characterization of the optimized plates

The resonant frequency was measured on each tactile plate. We found:

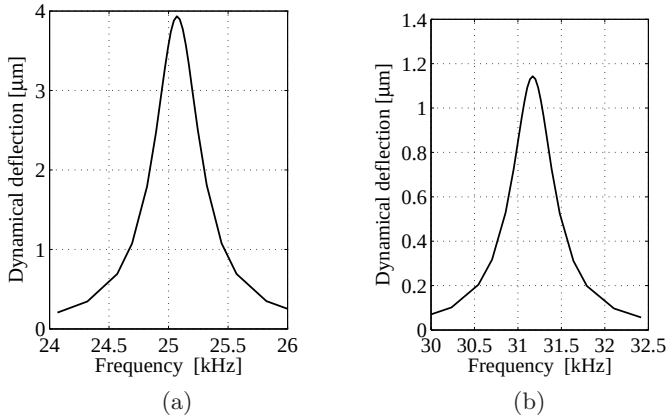

Figure 11: Time harmonic simulation (a) around 25070 Hz for the tactile plate with $h_\mathrm{p} = 0.5$ mm, $\lambda^* = 16.10$ mm, $h_\mathrm{i}^* = 0.500$ mm and (b) around 31170 Hz for the tactile cell with $h_\mathrm{p} = 1.0$ mm, $\lambda^* = 24.00$ mm, $h_\mathrm{i}^* = 2.0$ mm. The peak values correspond with Fig. 8and Fig. 5 respectively.

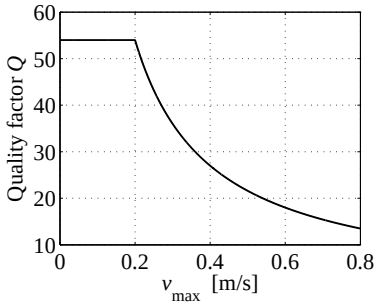

Figure 12: The quality factor decreases if the speed during resonance increases.

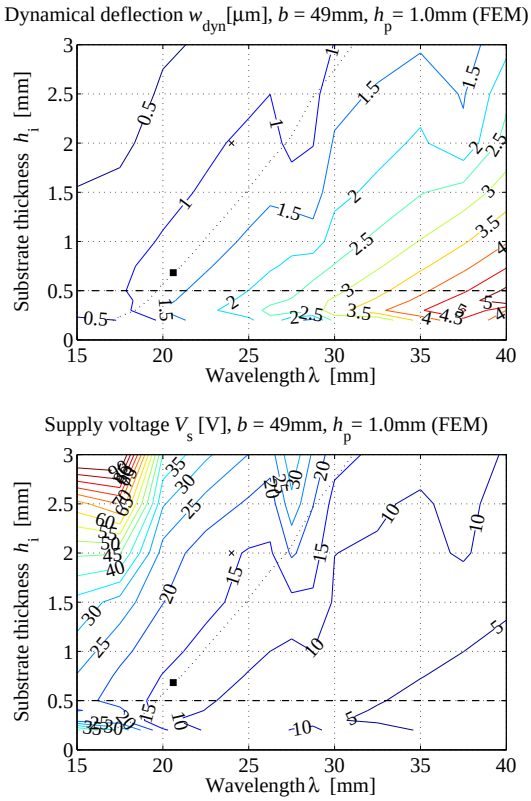

Figure 13: Contour lines of equal dynamical deflection in (a) and required voltage to obtain a deflection of 1.15 μm in (b) found by the numerical model for $h_\mathrm{p} = 1$ mm and Q-factor given in Fig. 12. The optimum $\lambda^* = 20.56$ mm, $h_\mathrm{i}^* = 6.73$ mm has the same position as in Fig. 5, but a lower $w_\mathrm{dyn} = 1.2731$ μm. The dashed line shows the configurations with $f_\mathrm{r} = 25$ kHz.

- for P1: $f_r = 23.160kHz$,
- for P2: $f_r = 23.950kHz$.

These figures don't exactly match the target value of the optimization process. However, the small shift observed is compatible with squeeze film effect: sensation may be softened but is still perceptible to human finger.

We also measured the dynamical deflection for the two plates, using a laser interferometer. We present in figure 16 the contour and a 3-d view of the same measurements for the plate P1. We also depicted the same plots for the plate P2 in figure 17. In order to avoid resonant frequency drift due to temperature rise during the run, measurements were done at low voltage level, and thus low vibration amplitude.

These figures show that the resonance mode found is the same for both plates, and the wavelength matches the value found for the optimization process. However, the two plates do not behave exactly the same. In fact, dynamical deflection of the big plate ($h_i = 0.75mm$,$h_p = 1.0mm$) is more disrupted than the thin one: tactile stimulation is not homogenous all over the plate, more particularly for the big plate. This problem is due to a transverse mode which resonance frequency is too close to the working frequency. Compared to the original plate, the transverse mode of the optimized plates has a more harmful effect, as shown in figure 18.

We finally measured the dynamical deflection of each plate as a function of the voltage supplied to the resonator. The results, presented in figure 19, show that the voltage which is necessary to attain the nominal deflection is lower for the thin plate than for the big one or the original tactile plate.

Thus, the optimized tactile plate needs less voltage to produce the same dynamical deflection, and requires less energy during operation. Best results are obtained with the thin plate because the required supply voltage is $6[V]$ only to produce $1.15\mu m$. This confirms the analytical conclusion of chapter 3.2, because for the same voltage amplitude, dynamical deflection reduces by increasing h_p.

5. Conclusion

This paper presents the optimization process of a tactile plate. Optimized plates require higher deflection for the same voltage level and a resonance frequency higher than $25kHz$ to allow squeeze film effect. We obtained

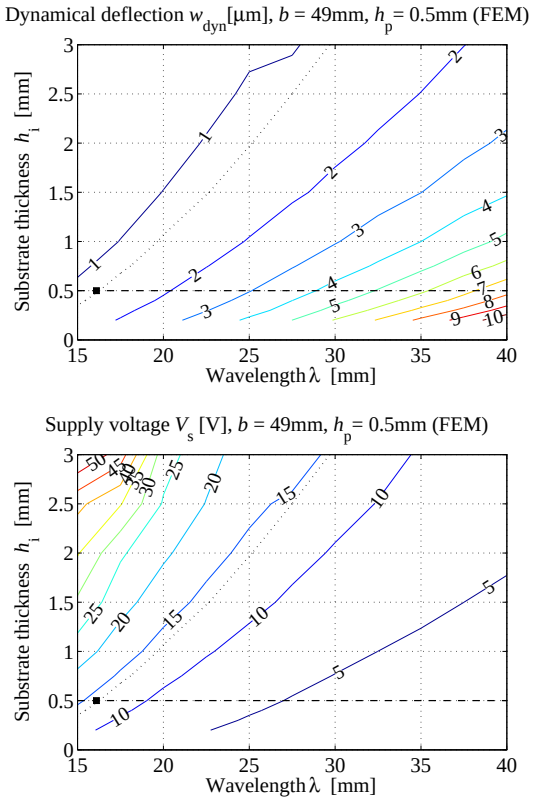

Figure 14: Contour lines of equal dynamical deflection in (a) and required voltage to obtain a deflection of 1.15 μm in (b) found by the numerical model for $h_{\rm p} = 0.5$ mm and Q-factor given in Fig. 12. The optimum $\lambda^* = 15.66$ mm, $h_{\rm i}^* = 0.500$ mm has almost the same position as in Fig. 8, but a lower $w_{\rm dyn} = 1.215$ μm. The dashed line shows the configurations with $f_{\rm r} = 25$ kHz.

Figure 15: A manufactured tactile plate made up with 28 piezo cells glued onto the copper beryllium plate.

two optimized plates which were manufactured and characterized. The new designs present more transverse mode than on the original plate configuration, and a resonance frequency slightly lower than the optimization condition. However, more deflexion at lower voltage level is obtained in return. The optimized plate with the thinner layer of piezo-ceramic offers better performances than the bigger one. Deflection is more homogenous over the tactile plate, and a supply voltage of $6[V]$ only is required to work at nominal deflection. This new design has an important

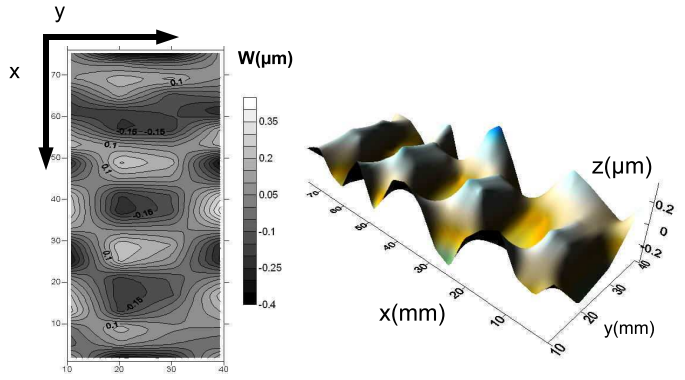

Figure 16: Measured dynamical deflection for the plate P1($h_p = 1.0mm$, $h_i = 0.75mm$ and $\lambda^* = 20.56mm$).

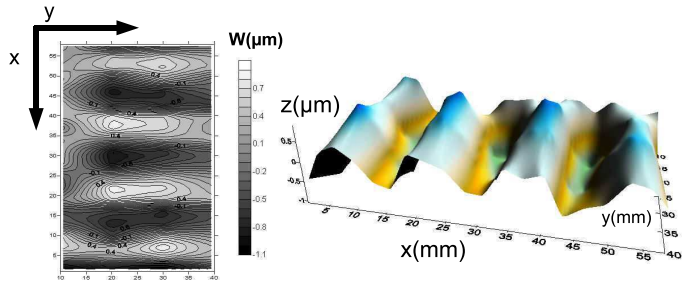

Figure 17: Measured dynamical deflection for the plate P2 ($h_p = 0.5mm$, $h_i = 0.5mm$ and $\lambda^* = 15.66mm$).

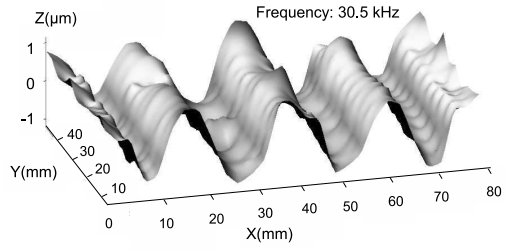

Figure 18: Measured dynamical deflection for the original plate configuration

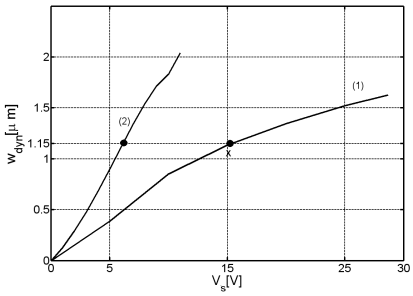

Figure 19: Measured dynamical deflection as a function of the supply voltage V_s (1) is for the plate P1($h_p = 1.0mm$, $h_i = 0.75mm$, $\lambda^* = 20.56mm$) and (2) is for P2($h_p = 0.5mm$, $h_i = 0.5mm$, $\lambda^* = 15.66mm$). The cross indicates the dynamical deflection of the original tactile plate

property: with such a low voltage, the tactile plate can be used in a computer environment more easily.

Acknowledgment

This work was carried out within the framework of the INRIA Alcove project and is supported by the IRCICA (Institut de Recherche sur les Composants logiciels et matériels pour l´Information et la Communication Avancée) and The European Commission (FEDER). Furthermore, this work was supported by the FWO project G.0082.06, by the GOA project BOF 07/GOA/006 and by the Interuniversity Attraction Poles (IAP) project P6/21. The first author is a postdoctoral researcher of the FWO.

References

[1] S.A. Wall, S. Brewster, Sensory substitution using tactile pin arrays: Human factors, technology and applications, Signal Processing *Special Section: Multimodal Human-Computer Interfaces* , vol.86 N 12 pages 3674–3695, 2006

[2] V. Hayward, J.M. Cruz-Hernandez, Tactile display device using distributed lateral sjin stretch, IMECE 2000 Conference, 5–10 nov. 2000

[3] T. Watanabe, S. Fukui, A method for controlling tactile sensation of surface roughness using ultrasonic vibration, IEEE Int. Conf. on Robotics and Automation, p. 1134– 1139, 1995

[4] M. Biet, G. Casiez, F. Giraud, B. Lemaire-Semail, Discrimination of Virtual Square Gratings by Dynamic Touch on Friction Based Tactile Displays, symposium on Haptic interfaces for virtual environment and teleoperator systems, 2008, Reno, 2008, p. 41 – 48

[5] L. Winfield, J. Glassmire, J.E. Colgate, and M. Peshkin, T-pad: Tactile pattern display through variable friction reduction in WorldHaptic, march 2007, Tsukuba, pp. 421-426.

[6] M. Biet, F. Giraud and B. Semail, Squeeze film effect for the design of an ultrasonic tactile plate, IEEE Transactions on ultrasonics, ferroelectrics, and frequency control, 54 (2007) 2678–2688.

[7] M. Doelle, D. Mager, P. Ruther, and O. Paul, Geometry optimization for planar piezoresistive stress sensors based on the pseudo-Hall effect, Sensors and Actuators A, 127 (2006) 261–269.

[8] V. Monturet and B. Nogarede, Optimal dimensioning of a piezoelectric bimorph actuator, Eur. Phys. J. Appl. Phys., 17 (2002) 107–118.

[9] H-C Chung, K.L Kummari, S.J. Croucher, N.J. Lawson, S. Guo, R.W. Whatmore, Z. Huang Development of piezoelectric fans for flapping wing application, Sensors and Actuators A vol. 149 (2009) 136-142.

[10] L. Landau and E. Lifchitz, Theory of elasticity, course of theoretical physics, 3rd Ed., Vol. 7, Butterworth-Heinemann, Oxford, UK, 1986.

[11] A. D. Nashif, D. I. G. Jones, and J. P. Henderson, Vibration damping, John Wiley & Sons, New York, 1985.

[12] J. L. Rose, Ultrasonic waves in solid media, Cambridge University Press, Cambridge, UK, 1999.

[13] K. F. Graf, Wave motion in elastic solids, Dover, Mineola, NY, 1991.

[14] J. W. Bandler, Q. S. S. Cheng, S. A. Dakroury, A. S. Mohamed, M. H. Bakr, K. Madsen, and J. Sondergaard, Space mapping: The state of the art, IEEE Trans. Microwave Theory and Techniques, 52 (2004) 337–361.

[15] P. Sergeant, L. Dupré and J. Melkebeek, "Space mapping method for the design of passive shields", Journal of Applied Physics, 99 (2006) Art. No. 08H901.

[16] L. Encica,J.L.G. Janssen, J.J.H. Paulides, E.A. Lomonova Electromagnetic Actuators for Gravity Compensation and Vibration Isolation, Sensor Letters, Vol. 7, N 3, June 2009 , pp. 360-363(4).

[17] K. Uchino, Piezoelectric actuators and ultrasonic motors, Kluwer Academic Publishers, Dordrecht, The Netherlands, 1997, p. 82.

Biography

Peter Sergeant was born in 1978. In 2001, he graduated in electrical and mechanical engineering at the Ghent University, Belgium. In 2006, he received the degree of Doctor in Engineering Sciences from the same university. He joined the Department of Electrical Energy, Systems and Automation, Ghent University in 2001 as Research Assistant. From 2006, he is postdoctoral researcher for the Fund of Scientific Research Flanders (FWO) at Ghent University, and since 2008 also researcher at University College Ghent. His main research interests are numerical methods in combination with optimization techniques to design nonlinear electromagnetic systems, in particular electromagnetic actuators and magnetic shields.

Frédéric Giraud was born in France in 1973. He graduated from Ecole Normale Supérieure de Cachan, France in 1996 and received the B.S. degree in electrical engineering from Paris-XI University, Orsay, France in 1995, the M.S. Degree in electrical engineering in 1997 from Institut National Polytechnique de Toulouse, France, and the phD degree from Lille University, in 2002. He's a member of the electrical engineering and power electronics laboratory of Lille (L2EP) as an Associate Professeur. His research deals with the modelling and the control of piezoelectric actuators used in mecatronic systems. Tactile is a new field of interest.

Betty Semail received her Ph. D degree in 1990 from University of Paris XI, Orsay and habilitation degree in 1997 from University of Science and Technology of Lille. Since 1990 she has been assistant professor in Ecole Centrale of Lille, till 1998 and she is now professor in University of Lille 1. She is a member of the electrical engineering and power electronics laboratory of Lille (L2EP) and responsible of the research axis upon control of electrical systems. She has been studying electromagnetic motors and now, her main field of interest deals with the modelling and control of piezo-electric actuators, for positioning and force feedback applications.